Turbulent Fluxes over Inhomogeneous Landscape①

Ye Zhuojia (叶卓佳), *Li Jun* (李 军) and *Fan Sihong* (范思泓)
LAPC, IAP, Chinese Academy of Sciences, Beijing 100029, China
Received August 21, 1996; revised October 31, 1996

ABSTRACT

Mesoscale surface turbulent fluxes over a complex terrain surrounded by oceans have been investigated using a 3-D numerical mesoscale model, under conditions with and without synoptic flows. The study indicated that under synoptically calm condition, the allocation and intensity of mesoscale surface turbulent fluxes (MSTFs) were greatly impacted by the thermally forced mesoscale circulation (TFMC) over mesoscale heterogeneous landscape. The maximum values of sensible (H_s) and latent (LE) heat fluxes were located over the convergent zones and considerably impacted by the soil wetness (M), but did not depend strongly on the atmospheric background thermal stability (β_0).

The simulated results suggested that the sensible heat flux was closely proportional to the square of wind speed in the surface layer. By the action of synoptic flow, the allocation of LE was shifted to downwind, its intensity increased.

Key words: Turbulent heat fluxes, Mesoscale circulation

I. INTRODUCTION

A grid interval in general circulation models (GCMs) is usually in the order of magnitude of 10^2 km. In the high resolution GCMs developed recently, the grid interval is in the order of 10^1 km. The minimal scale of resolved features in a numerical model is at least four times the grid intervals based on the suggestion from Pielke (1984) or even larger than eight grid intervals as argued by Grotch and MacCracken (1991). Therefore, the MSTFs, such as H_s and LE, can not be resolved in these GCMs. The improvement in weather forecast and the development of realistic climate change scenarios used GCMs require consideration of the impact of mesoscale heterogeneous landscape on MSTF's intensity and allocation.

Pielke (1974), Anthes (1984), Ookouchi et al. (1984), Segal et al. (1988), Ye et al. (1987, 1992, 1995a,b), and others manifested that non-classical mesoscale circulations (NCMCs) can be thermally forced over heterogeneous flat and complex landscapes. It can be anticipated that by the impact of the NCMCs, the intensity and allocation of MSTFs can be pronouncedly modified. In turn, weather and climate can be significantly adjusted. For better understanding the landscape-induced MSTFs and subsequent parameterizing them for the use in GCMs, Zeng and Pielke (1995) investigated the landscape-induced mesoscale H_s, LE and momentum fluxes using extensive 2-D numerical simulations over two types of surface configurations: alternating water and land strips and sinusoidal hills.

This study, using a 3-D regional atmospheric model, investigates the range of the MSTFs associated with these TFMCs, over complex terrain with topography and geography shown in Fig. 1a. The seasonal variation of the MSTFs under near calm condition was investigated in Section II. The impact of variation in M on the MSTFs will be illustrated in Section III. Section IV describes the possible impact of β_0 on the structures of the MSTFs. The

①This study was supported by Institute of Atmospheric Physics (IFA-CNR) at Roma, Italy.

synoptic flow influence on the MSTFs will be presented in Section V. Finally, conclusions drawn from the study will be described in Section VI.

II. SEASONAL VARIATION OF THE MSTFs

1. *A Brief Description of the Simulations*

The simulation domain was 300 km in north–south and 233 km in east–west, with a grid interval $\Delta x = \Delta y = 3.33$ km; the model consisted of 16 vertical levels, ranging from $z = 0$ to 13 km above the ground surface (AGS); the levels for potential temperature, θ, and specific humidity, q, in the air as well as the initial specific profile were presented in Table 2, which was typical in Calabria; the initial profile of θ was set to 2K / km for all cases except case 7; the synoptic flow for all cases was set to 0.5 m / s flowing from the south except for case 8, in order to isolate the impacts of variations in incoming solar radiation fluxes, M and β_0 on the MSTFs; there were 6 levels in soil model with a constant grid interval of 5 cm; the input soil parameters were described in Table 3; the initial wind fields were obtained by running the 3–D model to nearly steady state with the given initial specific humidity and potential temperature profiles; the simulations were run 12 hours beginning at 0800 local standard time (LST) with time step 15s.

Table 1. Description of the Numerical Model Simulations

Case	Synoptic Flow (m / s)		Simulated Day	M	β_0 (K / km)
1	$U_g = 0.0$	$V_g = 0.5$	Jul. 16	0.05	2.0
2	0.0	0.5	Oct. 16	0.05	2.0
3	0.0	0.5	Jan. 16	0.05	2.0
4	0.0	0.5	Jul. 16	0.20	2.0
5	0.0	0.5	Jul. 16	0.40	2.0
6	0.0	0.5	Jul. 16	1.00	2.0
7	0.0	0.5	Jul. 16	0.05	10.0
8	7.0	0.0	Jul. 16	0.05	2.0

2. *Seasonal Variation of MSTFs*

Figure 1 (b,c and d) presented X–Y cross sections of surface net radiation flux (R_n), H_s (with contour interval = 25 W / m^2 for R_n and 30.0 W / m^2 for H_s) and wind vector simulated at 1600 LST from case 1. Negative flux represents upward. Comparison between Figs. 1 b,c and d indicated that (a) there were three maximum negative values (MNVs) for R_n. One located above the Cosene river valley, between mountains H_3 and H_4. The other two located on south of mountain H_1 and north of mountain H_4, respectively, showing a complex, heterogeneous distribution for R_n; (b) from shore line into inland, both values of H_s and wind speed increased. H_s reached its maximum which was over wind convergent zone, caused by the collisions of head–on moving TFMCs. The allocations of the convergent zones and the MNVs for H_s seem to be well coincident. Above analysis explored that the value of H_s was considerably impacted by the TFMCs and their interactions.

Table 2. Numerical Model Levels for θ and q and Initial Profile of q

Z(km)	0.075	0.15	0.275	0.475	0.70	0.95	1.35	2.00
q	.011	.010	.009	.0075	.007	.003	.005	.002
Z(km)	2.80	3.60	4.50	5.75	7.25	9.0	11.5	13.0
q	.001	.0007	.0003	.00002	.00001	.00001	.00001	.00001

Table 3. Input Parameters for Soil Model

density	specific heat	conductivity
1.45 kg / m^3	0.35 cal / (cm^{3}K)	3.9 cm / s

Table 4. Extreme values of TFMC's winds (in m / s) in summer (S), winter (W) and autumn (A) for M = .05, 2 and 1.0, respectively

		(1)	(2)	(3)	(4)	M
S	u−	7.68 / −6.57	7.78 / −8.35	9.89 / −9.52	8.15 / −9.61	
	v−	7.50 / −6.68	8.38 / −6.97	8.99 / −7.06	8.54 / −9.05	0.05
	w−	1.200	1.020	1.560	1.490	
	R_n	−564	−525	−475	−475	
	H_s	−412	−361	−425	−411	
A	u−	6.40 / −5.39	5.50 / −6.13	6.85 / −6.81	6.55 / −6.29	
	v−	6.40 / −5.50	5.87 / −4.87	6.88 / −5.51	6.91 / −4.61	0.05
	w−	.970		.841	1.20	
	R_n	−365	−425	−361	−356	
	H_s	−226	−206	−239	−263	
W	u−	5.12 / −4.63	4.50 / −4.99	5.28 / −5.13	5.36 / −4.75	
	v−	5.00 / −4.50	5.12 / −3.00	5.63 / −4.39	6.27 / −4.24	0.05
	w−	.803		.641	.732	
	R_n	−320	−337	−320	1.12	
	H_s	−146	−138	−165	−198	
S	u−	6.88 / −5.74	6.79 / −7.00	8.23 / −8.01	7.75 / −7.84	
	v−	7.31 / −6.56	7.27 / −6.08	7.77 / −6.77	7.52 / −5.28	0.2
	w−	1.05	.879	1.05	1.31	
	H_s	−330	−278	−325	−334	
S	u−	5.28 / −4.72	4.95 / −5.12	5.51 / −6.18	5.63 / −5.59	
	v−	5.37 / −4.93	5.35 / −4.55	5.89 / −5.59	6.44 / −4.71	1.0
	w−	.809	.662	.829	1.08	
	H_s	−212	−159	−203	−216	

By comparing Figs. 1 c,e and f, the seasonal variation under synoptically calm condition can be seen clearly. It presents that the ratios in H_s computed between in summer and in winter ranged from 2.0 to 2.8, representing a possible annual variation in H_s under the given condition. However, the value of R_n in summer was only about 1.5 to 1.8 times as larger as that in winter at the given condition (see Table 4 for detail). It suggested that the annual variation of H_s is not uniquely dependent on R_n. The simulated TFMCs decreased from summer to winter as characterized by the extreme values of horizontal and updraft winds, illustrated

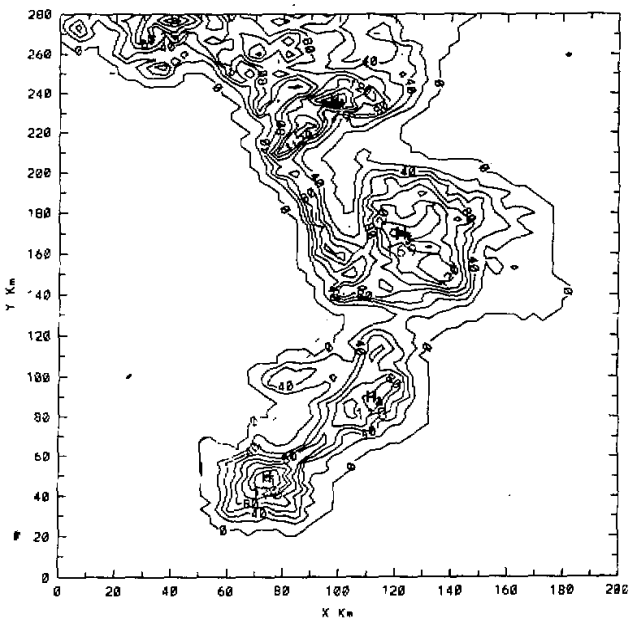
Y Km
X Km

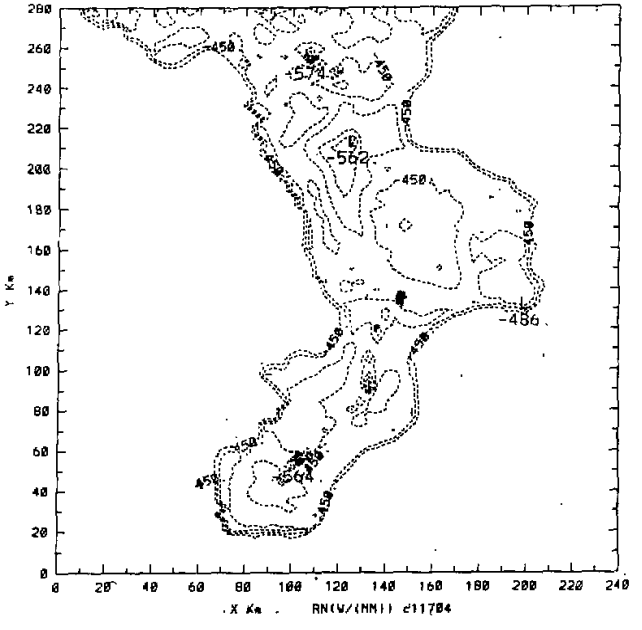
-574
-562
-486
Y Km
X Km
RN(W/(HM)) d11784

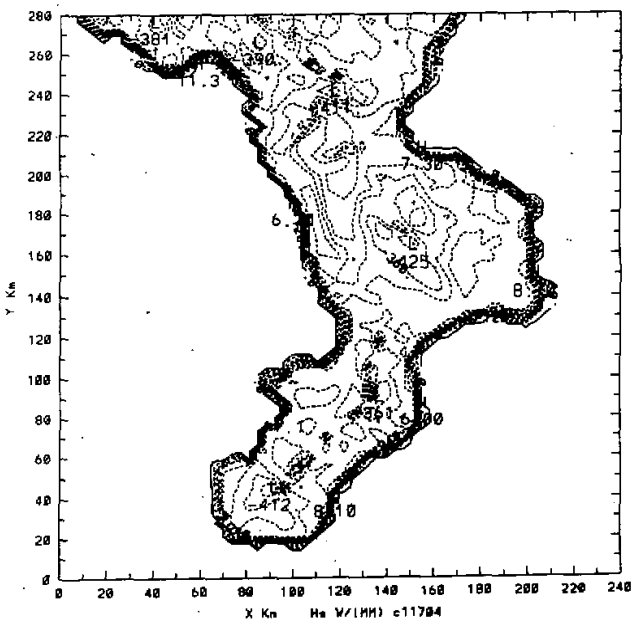
Y Km
X Km
Ha W/(MM) c11704

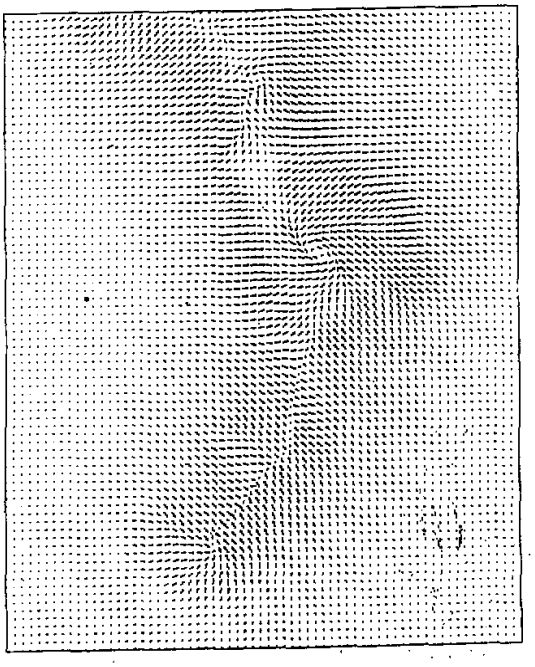

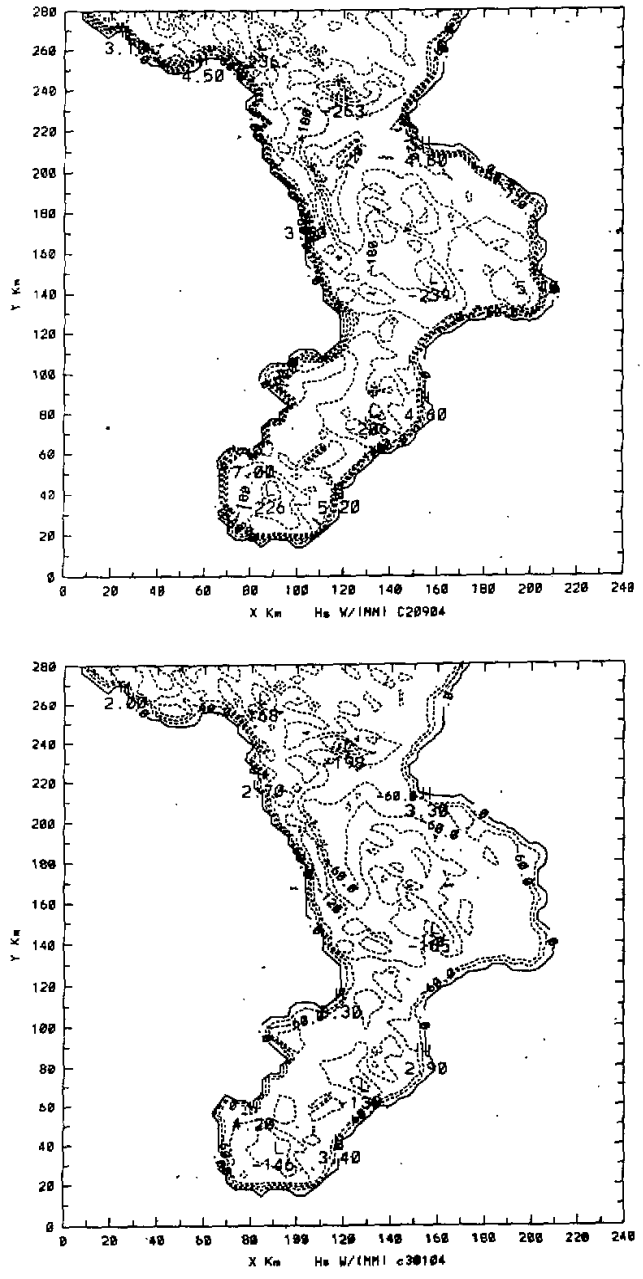

Fig.1 (a) The Calabria topography in Italy. H_1: Montalto; H_2: Pecoraro; H_3: Botte Donato; and H_4: Serra Dolcedorme; (b,c, and d) X−Y cross sections at 1600 LST for R_n, H_s and horizontal vector wind at 50 m above ground surface computed from case 1; (e and f) X−Y cross sections of H_s computed from cases 2 and 3.

in Table 4, where positive (on numerator) and negative (on denominator) value of u representing the TFMCs moving eastly and westly, respectively, and positive and negative value of v, northly and southly. It seems that the values of H_s and the TFMC's intensities have a close relationship as implied in Table 4 and shown in Table 5.

Line 3 in Table 5 means that the values of H_{s1} / u_1^2 were about equal to H_{s3} / u_3^2, indicating that H_s seems to be proportional to square of wind speed. The facts of annual variation greater in H_s than in R_n and the dependence of H_s on TFMC's intensity suggest that the turbulent intensity associated with the TFMCs plays a fundamental role in determination of MSTFs.

Results for H_s indicated above can be applied to the simulated values of LE. However, the annual variation in LE was stronger than that for H_s.

Table 5. The ratios of maximum H_s and u from case 1 (H_{s1}, u_1) and case 3 (H_{s3}, u_3) at 1600 LST

$A(H_{s1} / H_{s3})^{0.5}$	1.68	1.62	1.48	1.44
$B = u_1 / u_3$	1.50 / 1.42	1.73 / 1.67	1.87 / 1.86	1.52 / 2.02
A / B	0.9 / 0.8	1.1 / 1.0	1.3 / 1.3	1.1 / 1.4

III. THE IMPACT OF M ON TFMCs

Cases 4 to 6, together with case 1 were designed to study how the MSTFs would be altered when the value of M increased.

The simulated results for summer cases presented in Table 4 suggested that the MSTFs in H_s decreased when M increased. The simulated values of H_s in $M = 0.05$ were about two times as large as that in $M = 1.0$ (see Table 6 for detail). As opposed to H_s, the simulated value of LE sharply increased. The value of LE can reach to -518 W / m^2 for $M = 1.0$, but only -76 W / m^2 for $M = 0.05$. The maximum wind velocities decreased about 10% to 15% when M increased from 0.05 to 0.2, and 20% to 30% when M changed from 0.2 to 1.0. The dependences of simulated v– and w–component on M, similar to that indicated by u–component. The values of $(H_{s1} / H_{s6})^{0.5}$ and the ratios u_1 / u_6 for TFMCs eastward moving (numerator) and westward moving (denominator), respectively were also presented in Table 6. Line 3 in Table 6 also suggested that the values of H_{s1} / u_1^2, were about equal to H_{s6} / u_6^2, supporting the conclusion derived from the last subsection.

Table 6. Maximum values of H_s and u computed from cases 2 and 6 (indicated by subscripts 1 and 6) at 1600 LST

$A(H_{s1} / H_{s6})^{0.5}$	1.39	1.51	1.45	1.38
$B = u_1 / u_6$	1.45 / 1.39	1.57 / 1.54		1.45 / 1.72
A / B	1.0 / 1.0	1.0 / 1.0		1.1 / 1.2

IV. THE IMPACT OF β_0 AND H_s

Cases 1 ($\beta_0 = 2$ K / km) and 7($\beta_0 = 10$ K / km, representing very stable background atmosphere) were designed to study the possible impact of β_0 on TFMCs.

The simulated MSTFs reached to -308, -240, -310 and -327 (W / m^2), respectively, from case 7. About 40% decrement was simulated when the value of β_0 in case 7 was five

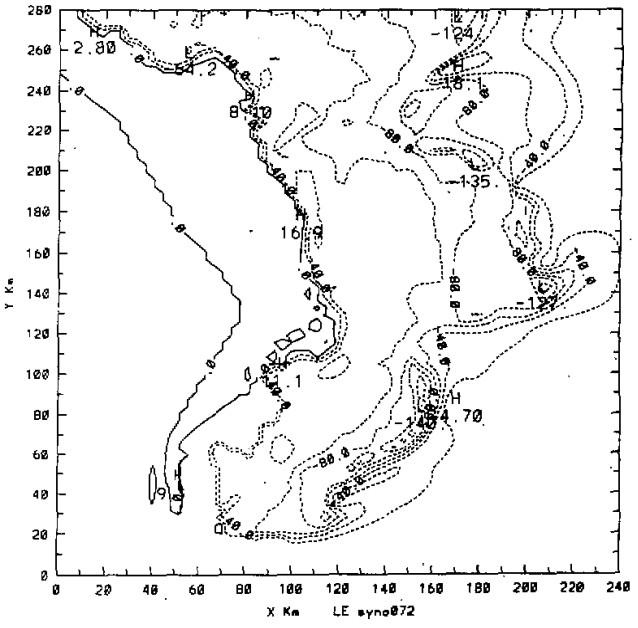
Y Km
X Km LE syno072

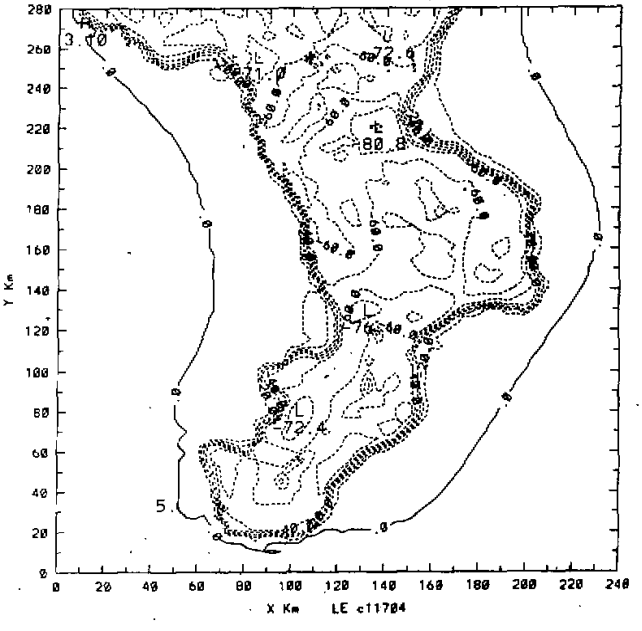
Y Km
X Km LE c11704

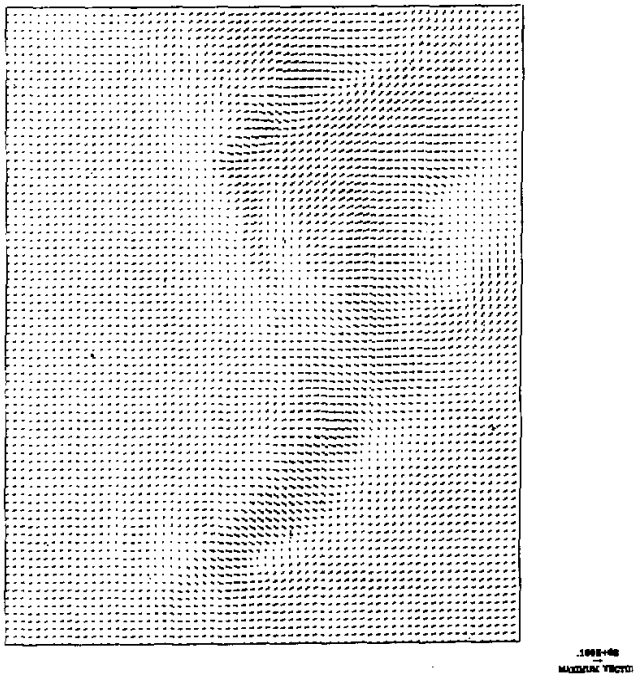

Fig. 2. Simulated terrain-followed X-Y cross sections of LE from case 8 (Fig. 2a) and from case 1 (Fig. 2b); wind vector at 50 m above surface from case 8 (Fig. 2c).

times as large as that in case 1, suggesting that H_s did not strongly depend on β_0.

V. THE IMPACT OF SYNOPTIC FLOW ON THE MSTFs

Case 8 and 1 were designed to study the impact of synoptic flow on the MSTFs. The allocation and intensity of LE simulated from case 8 were evidently different from that computed from case 1, with intensity increasing and MNVs of LE shifting to down-synoptic wind as shown in Figs 2a and 2b, simulated from cases 8 and 1, respectively. Simulation results also illustrated that by the interactions among the TFMCs, the synoptic flow and the topography, the four convergent zones, originally located over the land (see Fig. 1d), have been shifted to downwind (see Fig. 2c). That is the reason why the centres of LE in these cases have been moved to downwind by the action of synoptic flow.

VI. CONCLUSIONS

Using a 3-D numerical mesoscale model, the study investigated the mesoscale surface turbulent fluxes over a complex terrain surrounded by oceans under conditions with and without synoptic flow influence. The main conclusions were as follows.

* Under synoptically calm condition, the allocation and intensity of mesoscale surface turbulent fluxes were greatly impacted by the mesoscale circulation thermally forced over mesoscale heterogeneous landscape. The maximum values of sensible and latent heat fluxes were located over the convergent zones and considerably impacted by the soil wetness, but did not depend strongly on the background thermal stability.

* The simulated results suggested that the sensibly heat flux was closely proportional to the square of wind speed in the surface layer.

* By the action of synoptic flow, the allocation of LE was shifted to downwind, its intensity increased.

REFERENCES

Anthes, R.A. (1984), Enhancement of convective precipitation by mesoscale variations in vegetative covering in semiarid regions, *J. Climate Appl. Meteor.*, **23**: 541–554.

Grotch, C.M. and MacCracken, M.C. (1991), The use of general circulation models to predict regional climate change, *J. Climate*, **4**: 286–303.

Mahrer, Y and Pielke, R.A. (1977), A numerical study of the air flow over irregular terrain, *Cotrob. Atmos. Phys.*, **50**: 98–113.

McNider, R.T. and Pielke, R.A. (1981), Diurnal boundary layer development over sloping terrain, *J. Atmos. Sci.*, **38**: 2198–2212.

Ookouchi, Y., Segal, M., Kessler, R.C. and Pielke, R.A. (1984), Evaluation of soil moisture effects on the generation and modification of mesoscale circulation, *Mon. Wea. Rev.*, **112**: 2281–2292.

Segal, M., McCumber, M.C. and Pielke, R.A. (1988), Evaluation of vegetation effects on the generation and modification of mesoscale circulation, *J. Atmos. Sci.*, **45**: 2268–2292.

Pielke, R.A. (1974), A three-dimensional numerical model of sea breeze over South Florida, *Mon. Wea. Rev.*, **102**: 115–139.

Pielke, R.A. (1984), Mesoscale Meteorological Modeling, Academic Press, 612pp.

Ye Zhuojia, Segal, M. and Pielke, R.A. (1987), Effects of atmospheric thermal stability and slope steepness on the development of daytime thermally induced upslope flow, *J. Atmos. Sci.*, **44**: 3341–3354.

Ye Zhuojia and Jia Xinyuan (1992), A preliminary study on the impact of mesoscale irrigation over arid land on mesoscale climate, *Science in China (Series B)*, **35**: 1374–1384.

Ye Zhuojia and Jia Xinyuan (1995a), A numerical study on the impact of crop on mesoscale climate, *Science in China (Series B)*, **25**: 956–962 (in Chinese).

Ye Zhuojia and Jia Xinyuan (1995b), Mesoscale vegetation–breeze circulations and their impact on boundary layer structure at night, *Advances in Atmos. Sciences*, **12**: 29–46.

Zeng Xubin and Pielke, R.A. (1995), Landscape-induced atmospheric flow and its parameterization in large-scale numerical models, *J. Climate*, **8**: 1156–1177.